HHS Public Access

Author manuscript

Cancer Immunol Res. Author manuscript; available in PMC 2017 April 01.

Published in final edited form as:

Cancer Immunol Res. 2016 April ; 4(4): 323–336. doi:10.1158/2326-6066.CIR-15-0168.

NK Cell–Mediated Antitumor Effects of a Folate-Conjugated Immunoglobulin are Enhanced by Cytokines

Alena C. Jaime-Ramirez[#1], **Elizabeth McMichael**[#2], **SriVidya Kondadasula**[3], **Cassandra C. Skinner**[4], **Bethany L. Mundy-Bosse**[5], **Eric Luedke**[4], **Natalie B. Jones**[6], **Aruna Mani**[7], **Julie Roda**[8], **Volodymyr Karpa**[9], **Hong Li**[10], **Jilong Li**[10], **Saranya Elavazhagan**[11], **Krista M. La Perle**[12], **Alessandra C. Schmitt**[13], **Yanhui Lu**[14], **Xiaoli Zhang**[15], **Xueliang Pan**[15], **Hsaioyin Mao**[5], **Melanie Davis**[16], **David Jarjoura**[15], **Jonathan P. Butchar**[11], **Ming Poi**[10], **Mitch Phelps**[10], **Susheela Tridandapani**[11], **John C. Byrd**[16], **Michael A. Caligiuri**[5], **Robert J. Lee**[10], and **William E. Carson III**[2,4,5]

[1]Department of Neurosurgery, The Ohio State University, Columbus, OH

[2]Department of Biomedical Sciences Graduate Program, College of Medicine, The Ohio State University, Columbus, OH

[4]Department of Surgery, The Ohio State University, Columbus, OH

[5]Arthur G. James Comprehensive Cancer Center and Solove Research Institute, The Ohio State University, Columbus, OH

[10]College of Pharmacy, The Ohio State University, Columbus, OH

[11]Division of Pulmonary, Allergy, Critical Care and Sleep Medicine, Department of Internal Medicine, The Ohio State University, Columbus, OH

[12]Department of Veterinary Biosciences, College of Veterinary Medicine, The Ohio State University, Columbus, OH

[15]Center for Biostatistics, The Ohio State University, Columbus, OH

[16]Division of Hematology, The Ohio State University, Columbus, OH

[3]Karmanos Cancer Institute, Detroit, MI

[6]Riverside Breast Specialists, Westerville, OH

[7]Breast Cancer Center, Memorial Cancer Institute, Pembroke Pines, FL

[8]OncoMed Pharmaceuticals Inc., Redwood City, CA

[9]Wright State University School of Medicine, Dayton, OH

[13]Grady Memorial Hospital, Atlanta, GA

[14]Merck & Co, Kenilworth, NJ

[#] These authors contributed equally to this work.

Corresponding Author: William E. Carson, III, MD, Department of Surgery, N924 Doan Hall, 410 W. 10th Avenue, The Ohio State University, Columbus, OH 43210 Phone: (614) 293-6306 Fax: (614) 293-3465 william.carson@osumc.edu.

The authors have no conflicts of interest to disclose.

Abstract

Optimally effective antitumor therapies would not only activate immune effector cells, but engage them at the tumor. Folate-conjugated to immunoglobulin (F-IgG) could direct innate immune cells with Fc receptors to folate receptor–expressing cancer cells. F-IgG bound to human KB and HeLa cells, as well as murine L1210JF, a folate receptor (FR) overexpressing cancer cell line, as determined by flow cytometry. Recognition of F-IgG by NK cell Fc receptors led to phosphorylation of the ERK transcription factor and increased NK cell expression of CD69. Lysis of KB tumor cells by NK cells increased about 5-fold after treatment with F-IgG, an effect synergistically enhanced by treatment with IL2, IL12, IL15, or IL21 ($P < 0.001$). F-IgG also enhanced the lysis of chronic lymphocytic leukemia cells by autologous NK cells. NK cells significantly increased production of IFNγ, MIP-1α, and RANTES in response to F-IgG–coated KB target cells in the presence of the NK cell–activating cytokine IL12, and these coculture supernatants induced significant T cell chemotaxis $P < 0.001$). F-IgG–coated targets also stimulated FcR-mediated monocyte effector functions. Studies in a murine leukemia model confirmed the intratumoral localization and antitumor activity of F-IgG, as well as enhancement of its effects by IL12 ($P = 0.05$). The antitumor effect of this combination was dependent on NK cells and led to decreased tumor cell proliferation *in vivo*. Thus, F-IgG can induce an immune response against FR-positive tumor cells that is mediated by NK cells and can be augmented by cytokine therapy.

Keywords

Folate; Natural Killer Cell; Interferon-gamma; Immunoglobulin-G; IL12

Introduction

Folate is a water soluble B vitamin that functions as a cofactor in various cellular metabolic processes, such as nucleic acid synthesis and protein biosynthesis. Green vegetables, fresh fruits, and fortified foods are sources of folate (1). Cellular uptake of folate is mediated by at least three distinct transporters, which include the proton-coupled high affinity folate transporter, the reduced folate carrier (RFC), and the folate receptor (FR) (2). The proton-coupled high affinity transporter is a major folate transporter in low pH environments, such as the intestines, and appears to be the principal transporter in the gastric absorption of folate (3). The RFC, a bidirectional low-affinity transmembrane anion carrier, is ubiquitously expressed in normal tissues and is the predominant folate transporter in normal cells, but it will not transport folic acid (oxidized form) or folate conjugates (4). In contrast, the FR is a membrane bound high affinity unidirectional folate transporter protein that binds folic acid, chemical conjugates of folic acid, as well as folate-linked immunological agents. The FR has three well-established isoforms: α and β (both linked to glycosylphosphatidylinositol; GPI), and γ (5).

FR expression is normally low and limited to specific tissues, such as the choroid plexus, epididymis and kidney. In normal polar epithelial cells, the FR is predominantly located on the luminal (nonvascular) side of the cell. Thus, the FR expressed on normal cells is largely inaccessible to circulating folate or folate conjugates (5). The oncogenic potential of the FR

was first observed by Sidney Farber in 1948, where an accelerated leukemic process was observed in children treated with derivatives of folate (6). The FR is overexpressed on the surface of malignant cells, such as cancers of the cervix, breast, testes, and ependymal brain tumors (2, 7-9). This accessibility, relative to that of normal cells, makes the FR an attractive therapeutic target. Once a folate conjugate is bound, it may be taken up via endocytosis while a fraction remains engaged with the FR on the cell surface (5). These parameters are thought to create a favorable toxicity profile for folate-conjugated antitumor compounds (2).

NK cells are bone marrow–derived lymphocytes that can lyse malignant cells with altered expression of major histocompatibility antigens. NK cells express killer cell immunoglobulin receptors (KIRs), cellular adhesion molecules, and multiple cytokine receptors (e.g., receptors for IL12, IL15, and IL18). NK cells also produce several cytokines with antitumor effects (i.e., IFNγ, TNFα, and MIP-1α) and possess the ability to lyse malignant cells using cytolytic granules that contain perforin and granzymes. NK cells also express the FcγRIIIa (CD16) receptor, a low-affinity activating receptor that recognizes the constant (Fc) region of IgG. This receptor is critical in mediating antibody-dependent cellular cytotoxicity (ADCC) against antibody (Ab)-coated targets (10).

A folate-conjugated immunoglobulin (F-IgG) that is able to bind specifically to FR-bearing tumor cell lines was tested for its ability to mediate ADCC and cytokine production by NK cells. We also characterized the antitumor and immune effects of the F-IgG conjugate when used in combination with NK-activating cytokines that activate Fc receptor (FcR)-bearing NK cells.

Materials and Methods

Human and murine F-IgG synthesis

F-IgG (derived from all classes of IgG) and F-IgG-fluorescein isothiocyanate (FITC) were synthesized as described (11). Three folates per IgG were utilized for these studies. Unmodified human or murine IgG1 molecules were used as controls (C-IgG). The molecular weight of the F-IgG construct is approximately 151 kDa.

Cell lines

The FR^+ human cell lines KB (gift from Dr. Philip S. Low, Purdue University in 2006), HeLa, and F01 (human cervical and melanoma; ATCC obtained in 2002); OSU-NB and OSU-CLL (normal B and CLL cell lines, derived by J. Byrd from a CLL patient in 2012); and L1210JF (murine leukemia, gift from Robert J. Lee, Ohio State University in 2007); as well as the FR-negative cell line A549 (human alveolar adenocarcinoma; ATCC obtained in 2006) were propagated in folate-free RPMI 1640 (Invitrogen, Grand Island, NY) supplemented with 10% heat-inactivated fetal bovine serum (FBS) and 1% antibiotic-antimycotic. The identity of these cell lines was not authenticated by testing genomic DNA and cells were kept under passage number ten for all experiments.

Isolation of human NK, monocytes, and B cells

NK cells, monocytes, and B cells were isolated from fresh peripheral blood leukopacks (American Red Cross, Columbus, OH) or whole patient blood using RosetteSep cell specific cocktails (Stem Cell Technologies, Vancouver, BC) (12). Cells were cultured in folate-free RPMI 1640 (Cleveland Clinic Media Preparation Service, Cleveland, OH) supplemented with 10% heat-inactivated pooled human AB serum (HAB; C-Six Diagnostics, Germantown, WI) and 1% antibiotic-antimycotic. Normal donor NK cell Fc receptors (FcγRIIIa or CD16) were genotyped as described (13).

Reverse transcription polymerase chain reaction (RT-PCR)

Total RNA from KB, HeLa, and A549 cells was extracted in TRIZOL® Reagent using the RNeasy Mini Kit (Qiagen, Valencia, CA) following the manufacturer's protocol. RNA was converted to complementary DNA by reverse transcription and used as a template for RT-PCR using folate receptor alpha primers with the internal control 36B4 (14, 15).

Confocal microscopy and intra-tumoral flow cytometric analysis

KB tumor cells were treated with C-IgG– or F-IgG–FITC for 30 min at 37°C and collected at the designated time points. Cells were washed with flow buffer (5% FBS in PBS), fixed in 1% formalin in PBS, mounted on 25 × 75 × 1 mm slides (Erie Scientific, Portsmouth, NH) and stained with DAPI for nuclear identification (Vector Labs, Burlingame, CA) prior to analysis by immunofluorescence (IF) microscopy. Intracellular analysis of NK cell ERK phosphorylation was also assessed following coculture with KB tumor cells. NK cell activation was assessed 48 hours post coculture via FACS analysis with CD56-phycoerythrin (PE), CD158-allophycocyanin (APC), CD57-FITC, NKG2A-PE (Beckman Coulter, Brea, CA), CD56-APC, CD3-V450, CD16-FITC, NKG2D-APC, CD69–phycoerythrin-cyanin 7 (Pe-Cy7) and KIR/NKAT2-FITC, CD94-APC, NKp46/CD335-APC antibodies (BD Biosciences, San Jose, CA). In murine studies, IF microscopy of tumor sections was performed (16). Sections were analyzed on an Olympus Fluoview 1000 laser scanning confocal microscope. In murine studies with C-IgG– and F-IgG–FITC, tissues were harvested in the dark at indicated times. Tumors were dissociated (17) and stained with FR-α–APC (R&D Systems, Minneapolis, MN). $FR^+/FITC^+$ populations were assessed using a Becton Dickinson FACS Calibur flow cytometer (Becton-Dickinson, San Jose, CA) (16).

NK cell FcR stimulation assays and immunoblot analysis

Plates were coated with 50 μg/mL control IgG (C-IgG) or F-IgG overnight at 4°C then plated with NK cells. After 15 min at 37°C, cells were lysed in TN1 or 0.5% Brij-98 lysis buffer and probed with anti-phospho-ERK or ERK primary antibodies (Cell Signaling Technology, Beverly, MA), FR (FL-257, Santa Cruz Biotechnology, Santa Cruz, CA) or β-actin antibodies (Sigma, St. Louis, MO) (18).

Cytotoxicity assays

For ADCC assays, purified NK cells or monocytes were plated with medium supplemented with IL2 (10 ng/mL), IL12 (0.5 ng/mL or 10 ng/mL), IL15 (10 ng/mL), or IL21 (10 ng/mL). F-IgG or C-IgG-treated (100 μg/mL) ^{51}Cr-labeled target cells were added at various

effector:target (E:T) ratios for 4 h (NK cells) or 18 h (monocytes). Supernatants were harvested and ^{51}Cr was quantified (19).

In vitro coculture assay

KB and A549 cell lines were coated with F-IgG or C-IgG (100 μg/mL) and cocultured with NK cells or monocytes with medium containing IL2, IL12, IL15, IL18, or IL21 (10 ng/ml) (12). After 48 h, supernatants were analyzed for IFNγ, MIP-1α, TNFα, and RANTES content by ELISA and utilized in T cell chemotaxis experiments (20). For MDSC coculture experiments, MDSC were generated (21) and added to NK cell cocultures at a ratio of 0.5:1 MDSC:NK cell.

Murine tumor model

Mice were placed on a folate-deficient diet (AIN-90G, Dyets, Bethlehem, PA) one week prior to tumor cell injection (11). Age-matched, female DBA/2NCrl mice (Strain code 026; Charles River, Wilmington, MA) were injected with 10×10^6 L1210JF cells subcutaneously (s.c.). For intra-tumoral localization studies, age-matched, female athymic mice Crl:NU(NCR)-Foxn1^{nu} (Strain code 490; Charles River, Wilmington, MA) were inoculated with 4×10^6 human KB cells. Once tumors were palpable, mice were treated twice a week intraperitoneally (i.p.) with C-IgG or F-IgG (100 mg/kg), 2.5 ng mIL12 (Wyeth Pharmaceuticals, Madison, NJ), or the combination. Tumor volumes were assessed thrice weekly (16). To deplete monocytes/macrophages, 1 mg/kg of clodronate liposomes was administered on the day of tumor implantation and 0.5 mg/kg every four days thereafter (22). NK cells were depleted via anti-asialo GM1 (16).

Histological analysis of murine tissues

Murine tissues were harvested and processed immediately. Tumors were then sectioned and stained and quantified using the ScanScope XT and Positive Pixel Count Algorithm ImageScope software (Aperio Technologies) as described (16, 23).

Statistical Analysis

The synergistic effects of F-IgG and cytokines on NK cell mediated ADCC, IFNγ, or MIP-1α production were tested using linear mixed models to account for the correlated responses from the same cell types and the same donor cells. Treatment groups (C-IgG, F-IgG or the combination of C-IgG or F-IgG plus cytokines), E:T ratios were considered as a fixed effect. Ratios and treatment interactions were also included in the model. To control for type 1 error gate keeping strategies were used in each experiment at a significance level of 0.05, we first tested the difference between the combination treatments to the C-IgG treatment group (control) across different E:T ratios. If the difference was significant ($P < 0.05$), then the differences across different E:T ratios was further tested for the combination treatments versus F-IgG or C-IgG, and F-IgG versus C-IgG. The P values for each hypothesis was based on the corresponding interaction contrasts of the fixed effects parameters estimated from the linear mixed models using the Estimate or Lsmeans statement in the Proc Mixed procedure. T cell migration studies were analyzed using a two-way ANOVA with Turkey methods to correct for multiple comparisons. Changes in tumor volume over time were

assessed via a linear mixed model for longitudinal data. Tumor values were log-transformed in the model, and the differences in tumor volume were calculated at baseline and at the end of each study time points based on a linear mixed model. All data analyses were performed using the SAS V9.4 statistical software.

Results

Cell line FR-α expression

Both the human KB and HeLa tumor cell lines expressed the FR-α transcript, as indicated by RT-PCR (**Fig. 1A**), but not the A549 cell line. FR protein content was confirmed by immunoblot analysis in the HeLa, KB, and murine L1210JF cell lines (**Fig. 1B**). Surface expression of the FR was detected on the KB and L1210JF cell lines as determined by flow cytometry using a F-IgG-FITC labeled conjugate. The specificity of the interaction between F-IgG and the FR is supported by F-IgG binding inhibition in KB cells pretreated with folate (200 nM) (**Fig. 1C**). In addition, F-IgG–FITC binding was maintained for greater than 24 hours, as assessed by confocal microscopy, whereas C-IgG-FITC did not exhibit this binding (**Fig. 1D**). No FR was detected on NK cells (data not shown). Based on these experiments, the KB and L1210JF cell lines were utilized for *in vitro* and murine studies.

F-IgG activates NK cells

NK cells can interact with antibody-coated target cells via an activating, low-affinity Fc receptor (CD16), which can activate the MAPK/ERK signaling pathway (12, 19, 20). Stimulation of this pathway is critical for FcR-mediated NK cell lytic function and cytokine production. We hypothesized that binding of human NK cells to immobilized F-IgG would activate this pathway and result in the phosphorylation of ERK. As predicted, NK cells stimulated with F-IgG (or C-IgG) exhibited striking ERK activation at 15 minutes, as compared to the PBS-stimulated cells (**Fig. 2A**). NK cell ERK phosphorylation was also determined following exposure to F-IgG-coated tumor cells. An increase in the phosphorylation of ERK was observed in NK cells that were cocultured with F-IgG coated KB tumor cells after 45 minutes of treatment (**Fig. 2B**). CD69 upregulation on NK cells is associated with a productive antitumor response (24). CD69 expression on NK cells increased in response to F-IgG–coated tumor cells in both the CD56 bright and CD56 dim subsets (**Fig. 2C**). Activated NK cells also decreased CD16 expression when incubated with F-IgG, compared to C-IgG, an indication of Fc receptor occupation (data not shown) (25). No difference in the surface expression of NKG2D, CD57, NKp46/CD335 (activating receptors), CD158, NKG2A, CD94, or KIR/NKAT2 (inhibitory receptors) was observed (data not shown).

F-IgG treatment of FR^+ tumor cells enhances lysis

The effect of F-IgG on NK cell ADCC of FR^+ tumor targets was examined using KB tumor cells as targets in a standard 4 h ADCC assay with healthy donor human NK cells as effectors (19). NK cell-mediated ADCC with F-IgG coating of targets was significantly enhanced at all effector:target (E:T) ratios and in every donor tested, as compared to C-IgG ($P < 0.0001$) (**Fig. 2D**). F-IgG treatment did not enhance the lysis of the FR-negative cell line A549 (**Fig. 2E**). The difference in the average percent lysis between F-IgG and C-IgG

was significantly greater in the KB cell line as E:T ratios increased ($P < 0.001$) (**Fig. 2D**). This trend was not observed in A549 cells (**Fig. 2E**).

Cytokine enhancement of NK ADCC

Next, several NK cell–activating cytokines were evaluated for their ability to augment NK cell ADCC against F-IgG–treated KB tumor cells. NK cells were pretreated with cytokines (IL2, IL12, IL15, or IL21) and cocultured with F-IgG–coated tumor cells at various E:T ratios in a ^{51}Cr release assay (19). With every cytokine tested, F-IgG or cytokine-mediated lysis was significantly higher than that of C-IgG treatment alone (all $P < 0.01$). The combination of F-IgG and IL2 (**Fig 3A**), IL12 (**Fig. 3B**), IL15 (**Fig. 3C**), or IL21 (**Fig. 3D**) resulted in significantly higher tumor cell lysis than either F-IgG or cytokine treatment alone across all E:T ratios (all $P < 0.001$). A significant synergistic lysis effect was observed following treatment with every cytokine evaluated across different E:T ratios (IL2 $P = 0.001$, IL12 $P < 0.0001$, IL15 $P = 0.0017$, IL21 $P < 0.0003$). Next, FR blocking experiments were conducted in which the KB tumor cells were treated with varying amounts of folate to create high, medium, and low FR availability, and validated by flow cytometry (data not shown). NK cell ADCC was then assessed. As predicted, NK cell killing directly correlated with the level of available FR (**Supplementary Fig S1A**). In addition, NK cells from 8 normal donors were genotyped for CD16 variants and ADCC assays were conducted. The data for one representative F/F (lower affinity-Donor 3) and F/V donor (intermediate-Donor 7) are shown in (**Supplementary Fig. S1B**) (no high affinity V/V donors were identified). The expression of the intermediate affinity FcR by NK cells did not appear to confer an increased ability to conduct ADCC as compared to NK cells with the low affinity FcR (present in approximately 36% of the population) (26).

IL12 enhances lysis of F-IgG-treated CLL cells

Our group is also interested in immune-based approaches for the treatment of chronic lymphocytic leukemia (CLL). We therefore examined the effects of F-IgG in this context. The expression of the FR in CLL has been described (27) and was validated in CLL patients by our group (**Fig. 3E)**. The ability of CLL patient NK cells (TIL) to kill F-IgG–coated KB (**Fig. 3F**, left) or autologous CLL target cells (**Fig. 3F**, right) was determined in a standard ADCC assay, in which care was taken to remove FR-bound folate from target cells (28). Here, freshly isolated NK TILs from CLL patients mediated significant lysis against both targets and the cytolytic activity of these NK cells was markedly enhanced following stimulation with IL12 ($P < 0.0005$) (**Fig. 3F**).

IL12 enhances cytokine production and T cell migration

Costimulation of NK cells via the IL12R and CD16 leads to enhanced production of IFNγ due to colocalization of these receptors at cell membrane lipid rafts and subsequent enhancement of signal transduction (18). We hypothesized that NK cell–activating cytokines would enhance NK cell production of IFNγ following exposure to F-IgG–coated KB tumor cells. An *in vitro* assay was performed in which purified NK cells were cocultured with F-IgG-coated FR-positive tumor cells (12). KB (FR+) and A549 (FR-) cells were treated with F-IgG or C-IgG and plated with purified NK cells in the presence or absence of IL2, IL12,

IL15, IL18, or IL21. Supernatants were harvested 48 h later and assayed for IFNγ content. As was observed in the ADCC experiments, F-IgG treatment not only resulted in a significant increase in NK cell IFNγ secretion (all $P < 0.0001$), but also demonstrated a significant interaction with IL2, IL12, IL15, IL18, and IL21 ($P < 0.01$) (**Fig. 4A**). As the coactivation of the IL12R and CD16 can stimulate the secretion of other cytokines, the concentrations of MIP-1α and RANTES were also measured. NK cell production of MIP1-α (**Fig. 4B**) and RANTES (**Fig 4C**) was enhanced following treatment with F-IgG coated tumor cells and IL12, compared to C-IgG ($P < 0.0001$). Treatment of the FR^- cell line A549 with F-IgG did not enhance NK cell IFNγ production in response to any cytokine (data not shown).

NK cell–derived factors produced in response to immobilized IgG can serve as a powerful stimulus to T cell chemotaxis (20). As predicted, T cell chemotaxis was significantly enhanced upon exposure of T cells to coculture supernatants that were obtained following treatment of NK cells with F-IgG–coated tumor cells and IL12, compared to C-IgG ($P < 0.01$) (**Fig. 4D**). These results provide evidence that coadministration of cytokines with F-IgG can significantly enhance NK cell production of chemokines, which have the ability to recruit T cells to sites of inflammation. Human NK cells stimulated with F-IgG–coated tumor cells plus IL12 increased CD69 expression, a finding that is consistent with dual activation of the IL12R and FcR (**Fig. 4E**).

Induction of monocyte cytolytic activity and secretion of TNFα

Experiments were conducted to determine if F-IgG could enhance the effector functions of monocytes, another immune cell population that is critical to antibody-mediated immune responses (29). Lysis of FR^+ KB tumor cells by normal monocytes was significantly enhanced by pretreatment of the target cells with F-IgG ($P < 0.0001$), an effect that was further enhanced by activation of monocytes for 18 hours with IL12 (**Fig. 5A**). In addition, peripheral blood monocytes (PBM) secreted significantly large quantities of TNFα when exposed to plate- (**Fig. 5B**) and tumor-bound F-IgG (**Fig. 5C**), as compared to controls ($P < 0.001$). Monocytes also secreted IL12 in response to F-IgG–coated KB tumor cells (**Fig. 5D**) ($P < 0.04$). The role of monocytes in mediating the effects of F-IgG plus IL12 therapy were examined via the use of monocyte-depleting clodronate liposomes (22). Mice treated with clodronate liposomes bearing s.c. L1210JF tumors were treated twice a week via i.p. injections of 100 mg/kg murine C-IgG or F-IgG plus 2.5 ng murine IL12 and tumor volume was assessed. Depletion of monocytes/macrophage was confirmed by flow cytometric analysis, but this manipulation did not impact the efficacy of combination therapy (**Fig. 5E**). The difference between mock and clodronate depleted mice treated with F-IgG plus IL-12 was not significantly different. As other groups have indicated that exhausted or inhibited NK cells may have a negative impact on tumor growth control and survival (30, 31), we examined the potential role of myeloid-derived suppressor cells (MDSC) in modulating the NK cell response to F-IgG–coated tumor cells. Notably, overnight coculture of MDSC with human NK at a ratio of 0.5:1 significantly inhibited NK cell lysis of F-IgG–coated KB cells and also reduced the NK cell IFNγ secretion in response to this stimulus (**Supp. Fig. 2**). These results indicate that immune suppressor cells within the tumor microenvironment can impact the NK cell response to F-IgG–coated tumor cells.

Enhancement of murine NK cell cytotoxicity

We evaluated the cytotoxic potential of purified murine NK cells against F-IgG–coated L1210JF tumor cells in a ^{51}Cr-release assay (20). Folate was conjugated to a murine IgG molecule to create a murine F-IgG construct. Freshly isolated murine NK cells were cultured with low dose recombinant murine (rm) IL15 (0.5 ng/ml) (32), treated with medium alone or medium containing rmIL12 (10 ng/mL) and plated with L1210JF target cells. C-IgG or F-IgG–coated target cells were only minimally lysed by NK cells in the absence of cytokine treatment. In contrast, pretreatment of NK cells with IL12 significantly increased lysis of F-IgG–coated tumor cells at the 50:1 E:T ratio (13.05 ± 0.84% vs. 1.37 ± 0.77% lysis; $P < 0.05$).

Inhibition of tumor growth by IL12 plus F-IgG

Based on our *in vitro* findings, prior preclinical work from our laboratory, and the results of phase I clinical trials, we chose IL12 for further study (16, 33). The ability of the F-IgG conjugate to penetrate into the tumor microenvironment and specifically bind to tumor cells was evaluated. A F-IgG-FITC construct was utilized to assess its intratumoral penetration in a KB xenograft model. A strong fluorescence signal was detected 72 h later only in F-IgG–FITC treated mouse tumors (**Fig. 6A**, upper panel). Flow cytometric analysis confirmed that specific fluorescence was detectable only in FR$^+$ tumors (**Fig. 6A**, bottom panel). Even at this early time point, approximately 40% of the FR$^+$ tumor cells were targeted by F-IgG-FITC. A FR$^+$ murine leukemia tumor model was employed to determine whether IL12 could enhance the effect of an antitumor F-IgG construct in an immune competent model. Mice bearing s.c. L1210JF tumors were treated twice a week via i.p. injections of murine C-IgG or F-IgG (at 100 mg/kg), with or without murine IL12 (2.5 ng). No significant tumor volume differences were observed at baseline. However, by day 18 of treatment, the average tumor volumes of mice receiving either IL12 (453 ± 83 mm^3) or F-IgG alone (223 ± 68 mm^3) were significantly smaller than those of the C-IgG-treated mice (615 ± 152 mm^3) ($P < 0.05$). Mice that received the combination of IL12 and F-IgG had significantly smaller tumors (84 ± 43 mm^3) than those of mice receiving control treatments ($P = 0.05$) (**Fig. 5B**). Normal tissues from mice treated with F-IgG exhibited no histological damage (**Supp. Fig. 3**). These data demonstrate that the F-IgG conjugate specifically targets tumor cells, while sparing normal tissues *in vivo* and that IL12 can enhance the effects of F-IgG in a murine leukemia tumor model.

NK cells are required for the antitumor effects of IL12 and F-IgG

Based on our previous work, we hypothesized that NK cells were the key mediators of the tumor response mediated by IL12 plus F-IgG (16). Mice bearing s.c. L1210JF tumors were depleted of NK cells via anti-asialo GM1 antibodies, which resulted in > 97% NK cell depletion (data not shown). Mock-depleted mice received injections of an isotype-matched control antibody. Mice were then treated with IL12 plus F-IgG. Tumor growth was significantly inhibited in mock-depleted mice receiving IL12 and F-IgG ($P < 0.0001$). In contrast, treatment with F-IgG and IL12 had a minimal effect on tumor growth in the absence of NK cells (**Fig. 7A**). Activated intra-tumoral NK cells were observed only in the non-depleted treatment group (**Fig. 7B**). There was a marked inhibition of Ki67 in mice

receiving IL12 plus F-IgG, but not in NK cell depleted mice, as indicated by immunohistochemical staining (**Fig. 7C**). These data suggest that the antitumor effect of IL12 and F-IgG is dependent on NK cells.

Discussion

We have demonstrated that a F-IgG construct could bind to the FR of tumor cells. Tumor-bound F-IgG triggered the MAPK pathway in NK cells and coating FR-bearing tumor cells with F-IgG led to enhanced NK cell–mediated ADCC and CD69 expression. Pretreatment of NK cells with IL2, IL12, IL15, or IL21 enhanced ADCC beyond that observed with F-IgG alone. The addition of IL12 to the F-IgG stimulus resulted in robust production of IFNγ, MIP-1α, and RANTES by NK cells, significantly exceeding concentrations observed with either stimulus alone. Cytokines produced from the coculture of NK cells and FIgG coated tumor cells treated with IL-12 mediated significant T cell chemotaxis. The conjugate bound to FR^+ tumor cells *in vivo*, but normal tissues showed no obvious adverse effects. Administration of IL12 in combination with F-IgG elicited an antitumor response in a murine tumor model when compared to mice receiving IL12, F-IgG, or C-IgG alone. The antitumor effects of the combination therapy were dependent on NK cells and associated with reduced tumor cell proliferation. These results support the utility of administering cytokines with the F-IgG conjugate as a possible cancer therapeutic.

In murine models, the administration of high doses of folate is linked with tumor progression (34). Although it is not known whether FR-expression is needed by malignant cells, folic acid supplementation increases tumor cell growth and decreases patient survival in the context of FR^+ tumors (35). Conversely, a blockade of folate uptake decreases tumor cell proliferation, migration, invasion, and tumor burden, implicating folate in the survival, growth, and injury repair of malignant cells (34, 36-38). The reason for FR overexpression in tumor versus normal tissues remains elusive. It is possible that the FR might somehow confer a growth advantage by modulating folate uptake from serum, but direct evidence is lacking (39).

The present folate-IgG construct had binding and intracellular distribution characteristics in FR^+ cells that were similar to those of earlier radiolabeled folate-conjugated immunoglobulin constructs (40). Binding assays from studies conducted by Henriksen *et al.* estimated the binding affinity of a folate-conjugated immunoglobulin to be within the K_D range of 10^{-9} to 10^{-10} M, which is comparable to the reported high affinity binding of FRα for folic acid (K_D~ 10^{-9} M) (34). Biodistribution experiments using ^{125}I- and ^{211}At-labelled folate-immunoglobulin conjugates in Balb/C mice indicate that folate-conjugation to the antibody has a minor effect on the distribution of the conjugated antibody (40). Therefore, it is reasonable to conclude that the pharmacokinetic parameters of the present F-IgG would be similar to that of other therapeutic IgG-type monoclonal antibodies, including a relatively long half-life (days), low clearance (~0.5 L/d), and a small volume of distribution (approximate to the plasma volume) (41, 42). The present studies indicate that FR binding of F-IgG was evident as early as 30 minutes after treatment and retained on the cell surface for up to 24 hours *in vitro*. Moreover, *in vivo*, F-IgG was present in the tumor up to 72 hours after injection.

The FR has been previously utilized for the investigational delivery of cytotoxic drugs, radiopharmaceuticals, nanoparticles, liposomes, and immunotherapy (2, 13). Lu *et al.* showed that folic acid can carry a conjugated hapten to the tumor cell surface (the hapten forming a bridge between the cell surface FR and antibodies to it) and elicit primarily a T cell– and NK cell–based immune response to the tumor. This led to the generation and accumulation of autologous antibodies to haptens on the tumor surface, stimulating Fc receptor–bearing immune cells to mount an antitumor response against the opsonized tumor cells (43). The results of the present study suggest that the F-IgG construct is able to promote a direct interaction of FcR-bearing cells with FR-expressing cancer cells rather than relying on the induction of an Ab response.

Thompson *et al.* devised a method to specifically target T cells to FR overexpressing tumors utilizing a light-activated folate–anti-CD3 construct. Here, the folate portion of the construct binds to FR^+ cancer cells while the anti-CD3 portion binds T cells. Specific tumor targeting and T-cell binding was observed in a murine model (44). In contrast, the F-IgG construct described here can localize NK cells to tumor cells while simultaneously stimulating FcR-mediated effector functions. These studies support the development of FR-directed therapeutic immunoconjugates and suggest that co-administering cytokines would augment the activity of these reagents. The ability of F-IgG to mediate lysis of target cells derived from both leukemias and solid tumors speaks to the broad applicability of this therapeutic approach.

F-IgG–mediated ADCC was investigated in this study due to the importance of ADCC in the antitumor mechanisms of monoclonal antibody therapy (13, 45, 46). A study in patients receiving trastuzumab for $HER2/neu^+$ metastatic breast cancers demonstrated that ADCC plays a significant role in the antitumor response (46). Park *et al.* also demonstrated *in vivo* that the therapeutic effects of anti-HER2/neu antibody occur primarily through ADCC, lending further support to the theory that ADCC is an important mechanism by which antitumor monoclonal antibodies function (10, 45). We have previously shown that the dual engagement of NK cell CD16 and cytokine receptors by cytokines such as IL2, IL12, or IL21 results in synergistic ADCC and IFNγ production (12, 16, 19, 20, 33). We observed robust and synergistic increases in ADCC and the levels of IFNγ, MIP-1α, and RANTES produced by NK cells when they were exposed to the combination of IL12 and F-IgG–coated tumor cells, as compared to either stimulus alone. Supernatants from cultures of F-IgG and IL12-activated NK cells induced T-cell chemotaxis, highlighting the antitumor microenvironment provided by NK cell costimulation. Administration of IL12 in combination with F-IgG elicited a significant antitumor response that was NK cell-dependent in a murine tumor model. Thus, the coadministration of IL12 and the F-IgG construct could be expected to promote an NK-dependent antitumor response in the clinical setting.

Dual stimulation with IL12 and F-IgG stimulates NK cells to secrete MIP-1α and RANTES, factors that exert a strong chemotactic effect upon monocytes (47). Therefore, NK cell infiltration of F-IgG–treated tumor deposits might be followed by a wave of monocyte migration, especially in the presence of IL12, which further augments NK cell chemokine production. Conversely, monocyte-derived TNFα is a well known activator of NK cell cytolytic activity (48) and could potentially sensitize tumor targets to NK cell cytolytic

activity and apoptotic stimuli. The concurrent activation of NK cell and monocyte effector functions by IL12 and F-IgG has the potential to induce a synergistic antitumor immune response that relies upon the pre-programmed interdependence of these two innate immune cell populations.

Therapeutically, F-IgG may confer several advantages over other constructs. Studies of F-IgG localization *in vivo* demonstrate that the conjugate penetrates into the tumor microenvironment and specifically target tumor cells. About 40% of tumor cells are targeted by F-IgG after 72 h of treatment. This persistence may contribute to the ability of this agent to mediate tumor shrinkage. It is also possible that greater tumor targeting might be observed at later time points, with higher doses of F-IgG or that lower F-IgG binding was not detectable by flow cytometry. Specific engagement of tumor cell surface receptors, while sparing normal tissue, also results in a favorable toxicity profile, as demonstrated in this study. Being fully humanized, hypersensitivity reactions to F-IgG are unlikely to occur (49).

We have shown that F-IgG complexes can be utilized to specifically enhance immune responses by NK cells and monocytes against FR^+ malignancies. Treatment of NK cells and monocytes with immune stimulatory cytokines synergistically augmented their ability to lyse FR targeted tumor cells, *in vitro*. *In vivo*, the coadministration of IL12 and F-IgG resulted in significant tumor reduction, an effect that was dependent on the NK cell compartment. Thus, F-IgG and IL12 can selectively target NK cells to cancer cells by means of the FR.

Supplementary Material

Refer to Web version on PubMed Central for supplementary material.

Acknowledgments

Grant support: This work was supported by NIH Grants P01 CA95426, K24 CA93670, P30 CA16058 (W.E. Carson III, S. Tridandapani, J.C. Byrd, M.A. Caligiuri), T32 GM068412/F32 CA186542-01A1/Pelotonia Post Doctoral Fellowship (A.C. Jaime-Ramirez), T32 CA90338-27 (A. Mani), C.C. Skiner was a Pelotonia Fellow.

References

1. Stover PJ. Physiology of folate and vitamin B12 in health and disease. Nutr Rev. 2004; 62(6):S3–12. Pt 2. discussion S3. PubMed PMID: 15298442. [PubMed: 15298442]
2. Salazar MD, Ratnam M. The folate receptor: what does it promise in tissue-targeted therapeutics? Cancer Metastasis Rev. 2007; 26(1):141–52. PubMed PMID: 17333345. [PubMed: 17333345]
3. Qiu A, Jansen M, Sakaris A, Min SH, Chattopadhyay S, Tsai E, et al. Identification of an intestinal folate transporter and the molecular basis for hereditary folate malabsorption. Cell. 2006; 127(5): 917–28. PubMed PMID: 17129779. [PubMed: 17129779]
4. Matherly LH, Goldman DI. Membrane transport of folates. Vitam Horm. 2003; 66:403–56. PubMed PMID: 12852262. [PubMed: 12852262]
5. Lu Y, Low PS. Folate-mediated delivery of macromolecular anticancer therapeutic agents. Adv Drug Deliv Rev. 2002; 54(5):675–93. PubMed PMID: 12204598. [PubMed: 12204598]
6. Farber S, Diamond LK. Temporary remissions in acute leukemia in children produced by folic acid antagonist, 4-aminopteroyl-glutamic acid. N Engl J Med. 1948; 238(23):787–93. PubMed PMID: 18860765. [PubMed: 18860765]

7. Sudimack J, Lee RJ. Targeted drug delivery via the folate receptor. Adv Drug Deliv Rev. 2000; 41(2):147–62. PubMed PMID: 10699311. [PubMed: 10699311]
8. Hartmann LC, Keeney GL, Lingle WL, Christianson TJ, Varghese B, Hillman D, et al. Folate receptor overexpression is associated with poor outcome in breast cancer. Int J Cancer. 2007; 121(5):938–42. PubMed PMID: 17487842. [PubMed: 17487842]
9. Dhawan D, Ramos-Vara JA, Naughton JF, Cheng L, Low PS, Rothenbuhler R, et al. Targeting folate receptors to treat invasive urinary bladder cancer. Cancer Res. 2013; 73(2):875–84. PubMed PMID: 23204225. [PubMed: 23204225]
10. Takai T, Li M, Sylvestre D, Clynes R, Ravetch JV. FcR gamma chain deletion results in pleiotrophic effector cell defects. Cell. 1994; 76(3):519–29. PubMed PMID: 8313472. [PubMed: 8313472]
11. Li H, Lu Y, Piao L, Wu J, Yang X, Kondadasula SV, et al. Folate-immunoglobulin G as an anticancer therapeutic antibody. Bioconjug Chem. 2010; 21(5):961–8. PubMed PMID: 20429546. [PubMed: 20429546]
12. Parihar R, Dierksheide J, Hu Y, Carson WE. IL-12 enhances the natural killer cell cytokine response to Ab-coated tumor cells. J Clin Invest. 2002; 110(7):983–92. PubMed PMID: 12370276. [PubMed: 12370276]
13. Musolino A, Naldi N, Bortesi B, Pezzuolo D, Capelletti M, Missale G, et al. Immunoglobulin G fragment C receptor polymorphisms and clinical efficacy of trastuzumab-based therapy in patients with HER-2/neu-positive metastatic breast cancer. J Clin Oncol. 2008; 26(11):1789–96. PubMed PMID: 18347005. [PubMed: 18347005]
14. Simmons G, Rennekamp AJ, Chai N, Vandenberghe LH, Riley JL, Bates P. Folate receptor alpha and caveolae are not required for Ebola virus glycoprotein-mediated viral infection. J Virol. 2003; 77(24):13433–8. PubMed PMID: 14645601. [PubMed: 14645601]
15. van Meeuwen JA, Korthagen N, de Jong PC, Piersma AH, van den Berg M. (Anti)estrogenic effects of phytochemicals on human primary mammary fibroblasts, MCF-7 cells and their co-culture. Toxicol Appl Pharmacol. 2007; 221(3):372–83. PubMed PMID: 17482226. [PubMed: 17482226]
16. Jaime-Ramirez AC, Mundy-Bosse BL, Kondadasula S, Jones NB, Roda JM, Mani A, et al. IL-12 enhances the antitumor actions of trastuzumab via NK cell IFN-gamma production. J Immunol. 2011; 186(6):3401–9. PubMed PMID: 21321106. [PubMed: 21321106]
17. Held MA, Curley DP, Dankort D, McMahon M, Muthusamy V, Bosenberg MW. Characterization of melanoma cells capable of propagating tumors from a single cell. Cancer Res. 2010; 70(1):388–97. PubMed PMID: 20048081. [PubMed: 20048081]
18. Kondadasula SV, Roda JM, Parihar R, Yu J, Lehman A, Caligiuri MA, et al. Colocalization of the IL-12 receptor and FcgammaRIIIa to natural killer cell lipid rafts leads to activation of ERK and enhanced production of interferon-gamma. Blood. 2008; 111(8):4173–83. PubMed PMID: 18174382. [PubMed: 18174382]
19. Roda JM, Joshi T, Butchar JP, McAlees JW, Lehman A, Tridandapani S, et al. The activation of natural killer cell effector functions by cetuximab-coated, epidermal growth factor receptor positive tumor cells is enhanced by cytokines. Clin Cancer Res. 2007; 13(21):6419–28. PubMed PMID: 17962339. [PubMed: 17962339]
20. Roda JM, Parihar R, Lehman A, Mani A, Tridandapani S, Carson WE 3rd. Interleukin-21 enhances NK cell activation in response to antibody-coated targets. J Immunol. 2006; 177(1):120–9. PubMed PMID: 16785506. [PubMed: 16785506]
21. Lechner MG, Liebertz DJ, Epstein AL. Characterization of cytokine-induced myeloid-derived suppressor cells from normal human peripheral blood mononuclear cells. J Immunol. 2010; 185(4):2273–84. Epub 2010/07/21. doi: 10.4049/jimmunol.1000901. PubMed PMID: 20644162; PubMed Central PMCID: PMC2923483. [PubMed: 20644162]
22. Zeisberger SM, Odermatt B, Marty C, Zehnder-Fjallman AH, Ballmer-Hofer K, Schwendener RA. Clodronate-liposome-mediated depletion of tumour-associated macrophages: a new and highly effective antiangiogenic therapy approach. British journal of cancer. 2006; 95(3):272–81. Epub 2006/07/13. doi: 10.1038/sj.bjc.6603240. PubMed PMID: 16832418; PubMed Central PMCID: PMC2360657. [PubMed: 16832418]

23. Mundy-Bosse BL, Lesinski GB, Jaime-Ramirez AC, Benninger K, Khan M, Kuppusamy P, et al. MDSC inhibition of the IFN response in tumor-bearing mice. Cancer Res. 2011 PubMed PMID: 21680779.
24. Clausen J, Vergeiner B, Enk M, Petzer AL, Gastl G, Gunsilius E. Functional significance of the activation-associated receptors CD25 and CD69 on human NK-cells and NK-like T-cells. Immunobiology. 2003; 207(2):85–93. PubMed PMID: 12675266. [PubMed: 12675266]
25. Farag MM, Weigand K, Encke J, Momburg F. Activation of natural killer cells by hepatitis C virus particles in vitro. Clin Exp Immunol. 2011; 165(3):352–62. PubMed PMID: 21682720. [PubMed: 21682720]
26. Calemma R, Ottaiano A, Trotta AM, Nasti G, Romano C, Napolitano M, et al. Fc gamma receptor IIIa polymorphisms in advanced colorectal cancer patients correlated with response to anti-EGFR antibodies and clinical outcome. Journal of translational medicine. 2012; 10:232. Epub 2012/11/23. doi: 10.1186/1479-5876-10-232. PubMed PMID: 23171437; PubMed Central PMCID: PMC3551834. [PubMed: 23171437]
27. Shen F, Ross JF, Wang X, Ratnam M. Identification of a novel folate receptor, a truncated receptor, and receptor type beta in hematopoietic cells: cDNA cloning, expression, immunoreactivity, and tissue specificity. Biochemistry. 1994; 33(5):1209–15. PubMed PMID: 8110752. [PubMed: 8110752]
28. Xia W, Hilgenbrink AR, Matteson EL, Lockwood MB, Cheng JX, Low PS. A functional folate receptor is induced during macrophage activation and can be used to target drugs to activated macrophages. Blood. 2009; 113(2):438–46. PubMed PMID: 18952896. [PubMed: 18952896]
29. Shaw GM, Levy PC, LoBuglio AF. Human monocyte antibody-dependent cell-mediated cytotoxicity to tumor cells. J Clin Invest. 1978; 62(6):1172–80. PubMed PMID: 748372. [PubMed: 748372]
30. da Silva IP, Gallois A, Jimenez-Baranda S, Khan S, Anderson AC, Kuchroo VK, et al. Reversal of NK-cell exhaustion in advanced melanoma by Tim-3 blockade. Cancer immunology research. 2014; 2(5):410–22. Epub 2014/05/06. doi: 10.1158/2326-6066.CIR-13-0171. PubMed PMID: 24795354; PubMed Central PMCID: PMC4046278. [PubMed: 24795354]
31. Gill S, Vasey AE, De Souza A, Baker J, Smith AT, Kohrt HE, et al. Rapid development of exhaustion and down-regulation of eomesodermin limit the antitumor activity of adoptively transferred murine natural killer cells. Blood. 2012; 119(24):5758–68. Epub 2012/05/01. doi: 10.1182/blood-2012-03-415364. PubMed PMID: 22544698; PubMed Central PMCID: PMC3382935. [PubMed: 22544698]
32. Fehniger TA, Cai SF, Cao X, Bredemeyer AJ, Presti RM, French AR, et al. Acquisition of murine NK cell cytotoxicity requires the translation of a pre-existing pool of granzyme B and perforin mRNAs. Immunity. 2007; 26(6):798–811. PubMed PMID: 17540585. [PubMed: 17540585]
33. Parihar R, Nadella P, Lewis A, Jensen R, De Hoff C, Dierksheide JE, et al. A phase I study of interleukin 12 with trastuzumab in patients with human epidermal growth factor receptor-2-overexpressing malignancies: analysis of sustained interferon gamma production in a subset of patients. Clin Cancer Res. 2004; 10(15):5027–37. PubMed PMID: 15297404. [PubMed: 15297404]
34. Kelemen LE. The role of folate receptor alpha in cancer development, progression and treatment: cause, consequence or innocent bystander? Int J Cancer. 2006; 119(2):243–50. PubMed PMID: 16453285. [PubMed: 16453285]
35. Bottero F, Tomassetti A, Canevari S, Miotti S, Menard S, Colnaghi MI. Gene transfection and expression of the ovarian carcinoma marker folate binding protein on NIH/3T3 cells increases cell growth in vitro and in vivo. Cancer Res. 1993; 53(23):5791–6. PubMed PMID: 8242637. [PubMed: 8242637]
36. Oleinik NV, Krupenko NI, Krupenko SA. ALDH1L1 inhibits cell motility via dephosphorylation of cofilin by PP1 and PP2A. Oncogene. 2010; 29(47):6233–44. PubMed PMID: 20729910. [PubMed: 20729910]
37. Dudkowska M, Bajer S, Jaworski T, Zielinska J, Manteuffel-Cymborowska M, Grzelakowska-Sztabert B. Antifolate/folate-activated HGF/c-Met signalling pathways in mouse kidneys-the putative role of their downstream effectors in cross-talk with androgen receptor. Arch Biochem Biophys. 2009; 483(1):111–9. PubMed PMID: 19135973. [PubMed: 19135973]

38. Liu H, Huang GW, Zhang XM, Ren DL, J XW. Folic Acid supplementation stimulates notch signaling and cell proliferation in embryonic neural stem cells. J Clin Biochem Nutr. 2010; 47(2): 174–80. PubMed PMID: 20838574. [PubMed: 20838574]
39. Kane MA, Elwood PC, Portillo RM, Antony AC, Najfeld V, Finley A, et al. Influence on immunoreactive folate-binding proteins of extracellular folate concentration in cultured human cells. J Clin Invest. 1988; 81(5):1398–406. PubMed PMID: 3366900. [PubMed: 3366900]
40. Henriksen G, Bruland OS, Larsen RH. Preparation and preclinical assessment of folate-conjugated, radiolabelled antibodies. Anticancer research. 2005; 25(1A):9–15. Epub 2005/04/09. PubMed PMID: 15816513. [PubMed: 15816513]
41. Dostalek M, Gardner I, Gurbaxani BM, Rose RH, Chetty M. Pharmacokinetics, pharmacodynamics and physiologically-based pharmacokinetic modelling of monoclonal antibodies. Clinical pharmacokinetics. 2013; 52(2):83–124. Epub 2013/01/10. doi: 10.1007/s40262-012-0027-4. PubMed PMID: 23299465. [PubMed: 23299465]
42. Keizer RJ, Huitema AD, Schellens JH, Beijnen JH. Clinical pharmacokinetics of therapeutic monoclonal antibodies. Clinical pharmacokinetics. 2010; 49(8):493–507. Epub 2010/07/09. doi: 10.2165/11531280-000000000-00000. PubMed PMID: 20608753. [PubMed: 20608753]
43. Lu Y, Sega E, Low PS. Folate receptor-targeted immunotherapy: induction of humoral and cellular immunity against hapten-decorated cancer cells. Int J Cancer. 2005; 116(5):710–9. PubMed PMID: 15828051. [PubMed: 15828051]
44. Thompson S, Dessi J, Self CH. Preclinical evaluation of light-activatable, bispecific anti-human CD3 antibody conjugates as anti-ovarian cancer therapeutics. MAbs. 2009; 1(4):348–56. PubMed PMID: 20068406. [PubMed: 20068406]
45. Park S, Jiang Z, Mortenson ED, Deng L, Radkevich-Brown O, Yang X, et al. The therapeutic effect of anti-HER2/neu antibody depends on both innate and adaptive immunity. Cancer Cell. 2010; 18(2):160–70. PubMed PMID: 20708157. [PubMed: 20708157]
46. Varchetta S, Gibelli N, Oliviero B, Nardini E, Gennari R, Gatti G, et al. Elements related to heterogeneity of antibody-dependent cell cytotoxicity in patients under trastuzumab therapy for primary operable breast cancer overexpressing Her2. Cancer Res. 2007; 67(24):11991–9. PubMed PMID: 18089830. [PubMed: 18089830]
47. Fine JS, Byrnes HD, Zavodny PJ, Hipkin RW. Evaluation of signal transduction pathways in chemoattractant-induced human monocyte chemotaxis. Inflammation. 2001; 25(2):61–7. Epub 2001/04/26. PubMed PMID: 11321360. [PubMed: 11321360]
48. Matossian-Rogers A, Browne C, Turkish M, O'Byrne P, Festenstein H. Tumour necrosis factor-alpha enhances the cytolytic and cytostatic capacity of interleukin-2 activated killer cells. British journal of cancer. 1989; 59(4):573–7. Epub 1989/04/01. PubMed PMID: 2785398; PubMed Central PMCID: PMC2247151. [PubMed: 2785398]
49. Amos SM, Duong CP, Westwood JA, Ritchie DS, Junghans RP, Darcy PK, et al. Autoimmunity associated with immunotherapy of cancer. Blood. 2011 PubMed PMID: 21531979.

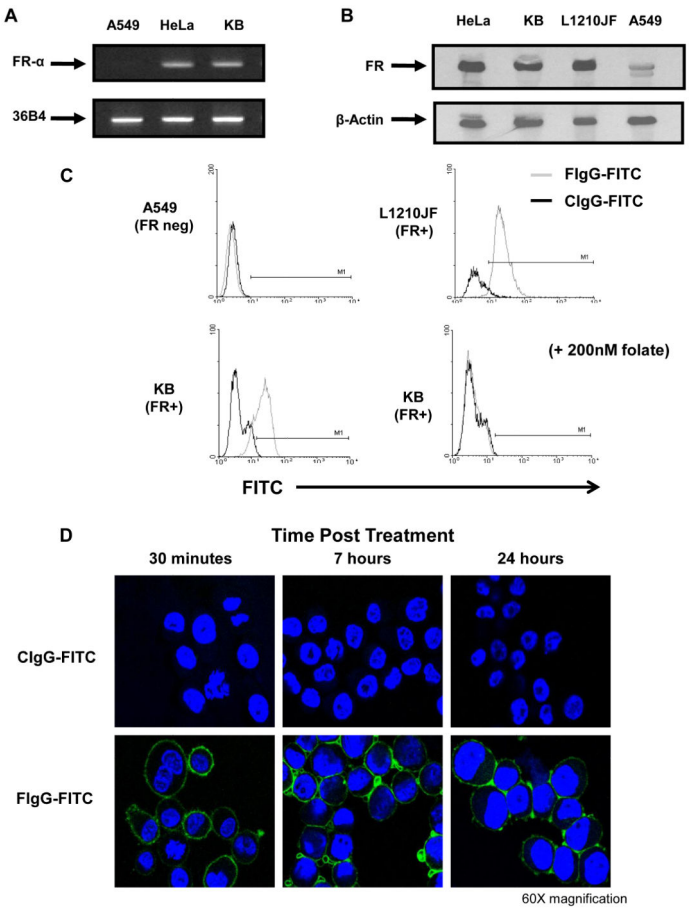

Figure 1. The folate receptor is expressed in HeLa and KB cells but not in A549 cells

(A) The FR-negative cell line A549 and the FR-positive cell lines HeLa and KB were tested for FR-α expression by RT-PCR., The internal control was 36B4 ribosomal RNA, present in all tumor cell lines. **(B)** Folate receptor expression was confirmed by immunoblot analysis in the HeLa, KB, and L1210JF cell lines. The membrane was reprobed for β actin to confirm equal loading. **(C)** FR expression by the A549 and L1210JF (top) and KB (bottom) cell lines was evaluated by flow cytometry using a F-IgG–FITC conjugate (200 nM, FIgG-FITC = gray histogram) or a FITC-labeled control Ab (CIgG-FITC = black histogram). As a control in the KB cell line, free folate was used to block the FR prior to labeling (bottom right panel). **(D)** F-IgG–FITC binding (green) to KB tumor cells was confirmed at various time points via confocal microscopy (60X magnification). Tumor sections counterstained with DAPI for nuclear identification (blue). Results shown are representative of at least three independent experiments.

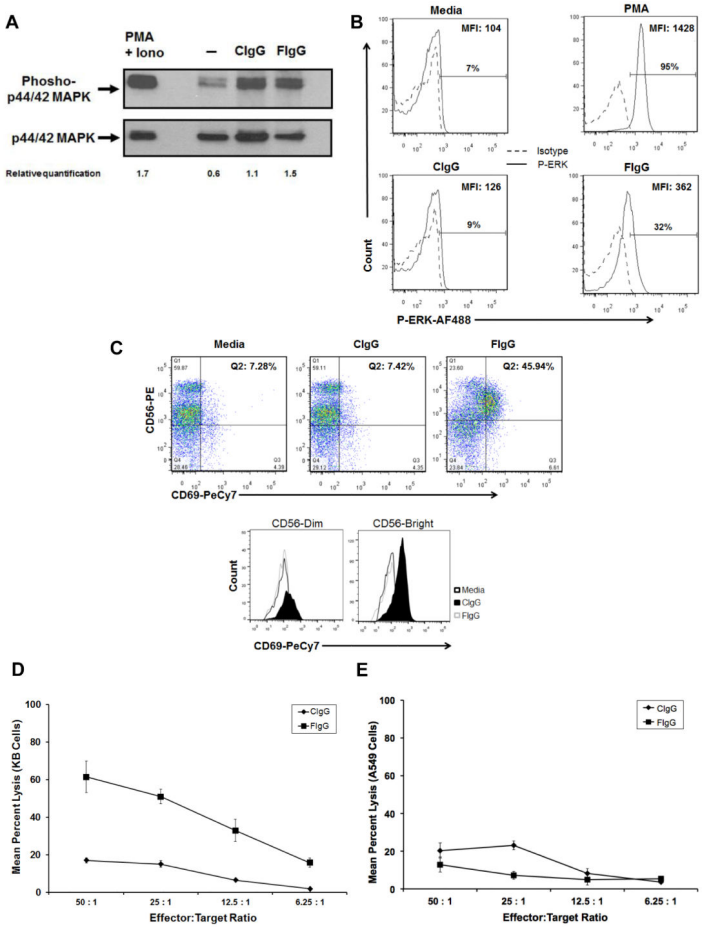

Figure 2. Phospho-ERK upregulation and cytolytic activity of NK cells in response to F-IgG stimulation

(A) Assessment by immunoblot. Freshly isolated NK cells were plated on immobilized C-IgG or F-IgG at 37°C for 15 minutes. Control conditions consisted of NK cells treated with PBS or PMA (positive control). NK cells were harvested and lysed for immunoblot analysis of phospho-ERK. Total ERK was measured as a loading control and relative quantification of P-MAPK vs ERK are indicated. **(B)** Assessment by intracellular flow cytometry. NK cells were stimulated with media, PMA, C-IgG or F-IgG coated KB tumor cells for 45 minutes and levels of phospho-ERK were determined by flow cytometry **(C)** Flow cytometry analysis of CD56/CD69 populations of NK cells. . Dual positive $CD56^{+}/CD69^{+}$ cells represent activated NK cells. The mean fluorescence intensity (MFI) of CD69 on both $CD56^{dim}$ and $CD56^{bright}$ cells was also determined for media (71.5 vs 77.4 MFI), CIgG (71.9 vs 66.5 MFI) and FIgG (165 vs 303 MFI) treated cells (bottom). The lytic activity of purified NK cells against C-IgG– or F-IgG–coated (D) FR^{+} tumor cells (KB cells) or **(E)** FR^{-} tumor cells (A549) was assessed in a standard 4-h chromium release assay: For KB targets, cytotoxic activity at all E:T ratios against F-IgG–coated cells differed significantly from C-IgG–coated KB cells, $P < 0.0001$, but A549 cells showed no significant differences. Results shown are representative of NK cells derived from $n = 4$ donors.

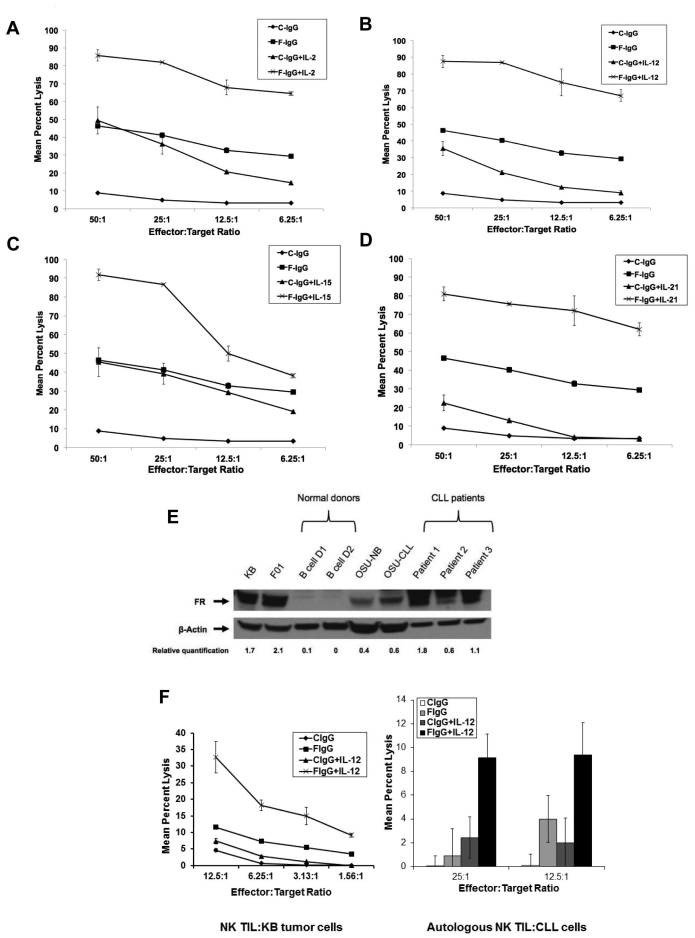

Figure 3. F-IgG NK cell mediated lysis is enhanced by cytokines

The lytic activity of cytokine-activated NK cells was assessed in a standard 4-hr chromium release assay in the presence of C-IgG or F-IgG coated KB tumor cells. Purified NK cells were incubated overnight with medium alone or medium supplemented with **(A)** IL2 (10 ng/mL), **(B)** IL12 (0.5 ng/mL), **(C)** IL15 (10 ng/mL), or **(D)** IL21 (10 ng/mL) at various E:T ratios (combinatorial F-IgG plus cytokine treatment groups all had significantly higher lysis at all E:T ratios, compared to C-IgG (all $P < 0.001$). **(E)** Folate receptor expression was confirmed by immunoblot analysis in the KB and F01 cell lines (positive controls), normal B cell donors ($n = 2$), OSU-NB and OSU-CLL cell lines, and CLL patient samples. The membrane was reprobed for β actin to confirm equal loading and relative quantification of FR vs β-actin are indicated. **(F)** The lytic activity of freshly isolated CLL patient NK cells (TIL) stimulated with IL12 (10 ng/mL) in the presence of C-IgG or F-IgG coated KB tumor cells (left) or autologous CLL cells (right panel), determined in a standard ADCC assay (combinatorial treatment was significantly higher than C-IgG at all E:T ratios ($P < 0.0005$). Results are representative of data derived from $n \geq 3$ donors/patients.

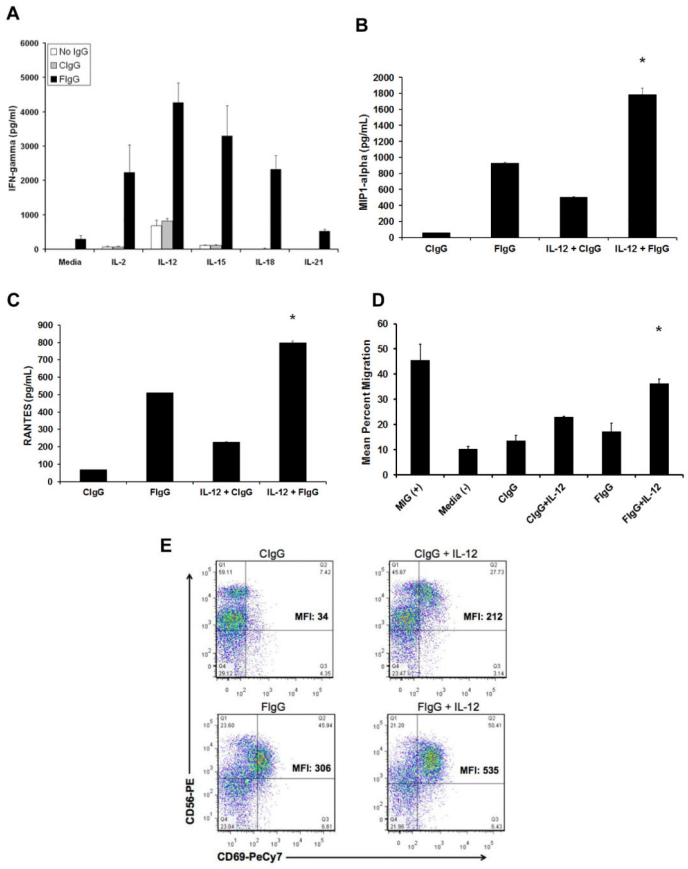

Figure 4. Human NK cells activated in response to F-IgG-coated KB cells and cytokines secrete IFNγ, MIP-1α, and RANTES and become motile

(A) NK cells were cocultured with F-IgG–coated KB tumor (FR-positive) cells in the presence of IL2, IL12, IL15, IL18, or IL21. Control conditions consisted of media only or C-IgG–coated tumor cells in the presence of the cytokines. Culture supernatants were harvested after 48 hours and analyzed for **(A)** IFNγ, **(B)** MIP-1α, and **(C)** RANTES by ELISA. Ccombinatorial treatment resulted in significant cytokine/chemokine production ($P < 0.0001$). **(D)** T cell chemotaxis was assessed with coculture supernatants. MIG treatment of media served as a positive control for T cell migration. (*) Indicates significant enhancement as compared to all other treatment groups except MIG ($P < 0.01$). **(E)** Activated NK cells were assessed via flow cytometric analysis for CD56 and CD69. Results are representative of data derived from $n \geq 2$ donors.

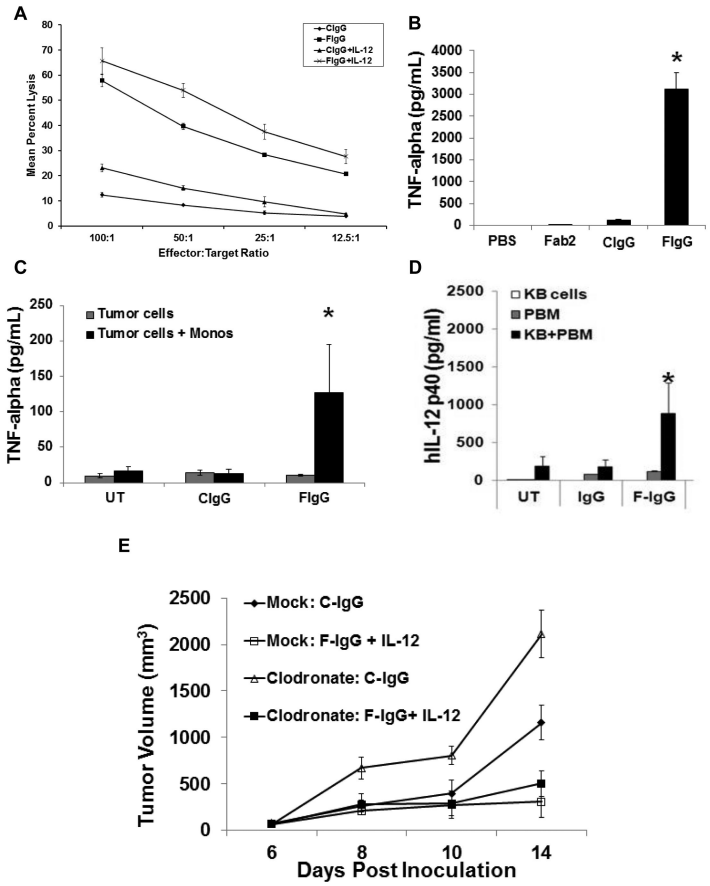

Figure 5. F-IgG plus IL12 enhances monocyte effector functions *in vitro* but not *in vivo*

(A) The lytic activity of freshly isolated normal monocytes stimulated with IL12 (10 ng/mL) in the presence of C-IgG or F-IgG coated KB tumor cells was determined in a standard 18 hour ADCC assay (combinatorial treatment was significantly higher than C-IgG or F-IgG at all E:T ratios with a $P < 0.001$). Normal monocytes were cultured with **(B)** plate-bound F-IgG or **(C)** F-IgG coated FR^+ KB tumor cells and culture supernatants were harvested after 48 hours then analyzed for TNFα and **(D)** IL12 by ELISA (* indicates $P < 0.04$). Results shown are representative of $n \geq 3$ donors. **(E)** Mice depleted of monocytes/macrophages bearing subcutaneous L1210JF tumors were treated once every 4 days with murine C-IgG (100 mg/kg) or F-IgG (100 mg/kg) plus murine IL12 (2.5 ng).

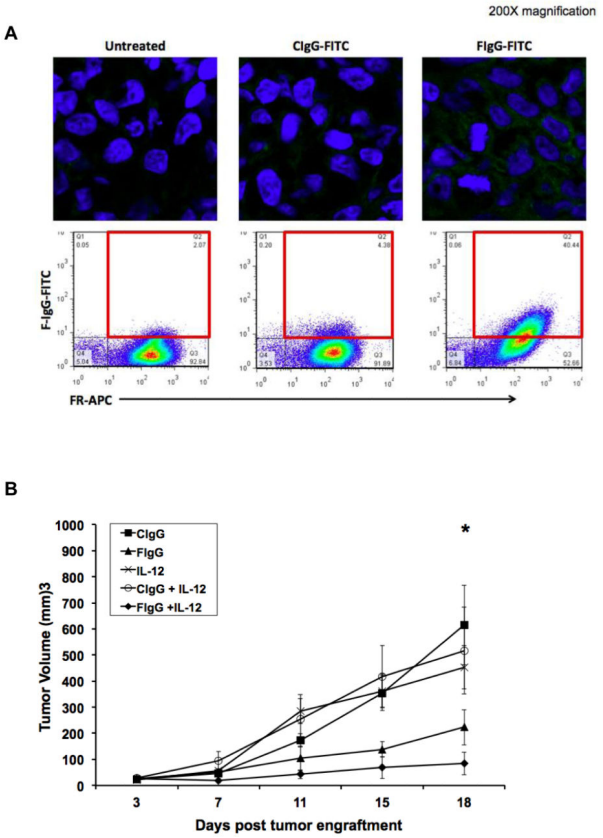

Figure 6. F-IgG binds to KB cell *in vivo* and IL12 enhances its antitumor effects in a murine model

(A) Mice bearing KB tumors were treated with 100 mg/kg CIgG-FITC or FIgG-FITC and sacrificed after 72 hours. Tumors were harvested and fixed/frozen or dissociated. FITC content (green) was assessed in fixed/frozen tissues via confocal microscopy (top panels). Nuclei are stained blue with DAPI (200X images). FR status and FITC content were then measured via flow cytometric analysis (bottom panels). Dual positive $FR^+/FITC^+$ cells indicate specific binding of F-IgG to FR^+ tumor cells. **(B)** Mice bearing subcutaneous L1210JF tumors were treated once every 4 days with 100 mg/kg murine C-IgG, 100 mg/kg murine F-IgG, 2.5 ng murine IL12, C-IgG plus IL12 or F-IgG plus IL12. Data is representative of $n = 3$ independent experiments. No significant differences in tumor volume were found between the five groups at baseline. However, at 18 days after treatment, the average tumor volumes of mice receiving either IL12 or F-IgG alone were smaller than those of the C-IgG-treated mice ($*P \leq 0.05$).

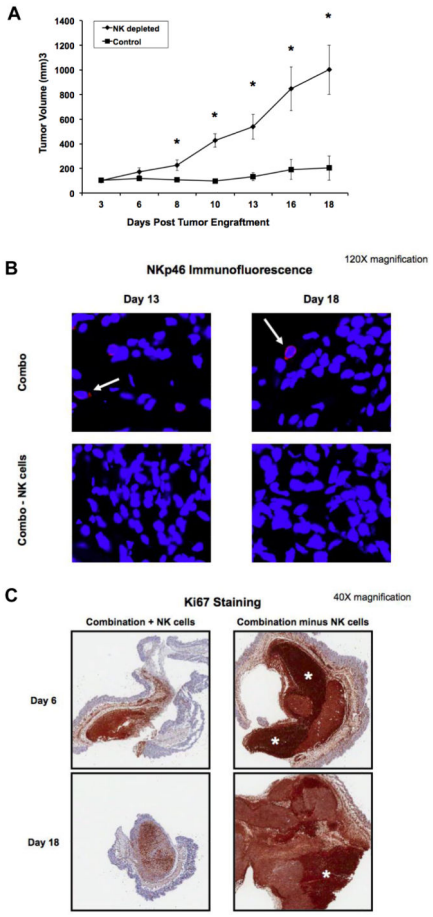

Figure 7. The antitumor effects of F-IgG plus IL12 are dependent on NK cells and result in decreased tumor cell proliferation

(A) Mice bearing subcutaneous L1210JF tumors were depleted of NK cells with an antibody to the asialo moiety, or treated with an istoype control antibody. $n \geq 4$ mice/group were treated with F-IgG (100 mg/kg) and IL12 (2.5 ng). $*P \leq 0.05$. **(B)** Confocal microscopy (120X) detected activated NK cells ($NKp46^+$ red stain) only in nondepleted mice (top, white arrow). Tumor sections were counterstained with DAPI for nuclear identification (blue). **(C)** Mice were sacrificed at the indicated time points and whole tumors were harvested and sectioned to measure tumor cell proliferation by Ki67 staining (5X). Scale bar indicates 800 um. White asterisks indicate areas of high Ki67 staining within the tumor. Data is representative of $n = 3$ independent experiments.